ARTICLES

Photophysical Characterization of Free-Base N-Confused Tetraphenylporphyrins

Jeffery P. Belair,[†] Christopher J. Ziegler,*[,†] Cheruvallil S. Rajesh,[‡] and David A. Modarelli*[,‡]

Department of Chemistry and The Center for Laser and Optical Spectroscopy, Knight Chemical Laboratory, The University of Akron, Akron, Ohio 44325-3601

Received: January 28, 2002; In Final Form: April 26, 2002

We report the photophysical characterization of the two tautomers (**1e** and **1i**) of 5,10,15,20-tetraphenyl N-confused free-base porphyrin, potential building blocks in assemblies designed for artificial photosynthesis, using a combination of steady state and time-resolved techniques. Tautomer **1e** was found to have a significantly higher quantum yield of fluorescence than tautomer **1i** ($\Phi_{Fl} = 0.036$ vs $\Phi_{Fl} = 0.0016$, respectively), despite the fact the fluorescence lifetimes were quite similar (i.e., 1.98 ns vs 1.60 ns, respectively). These differences were attributed to a more rapid rate of internal conversion or intersystem crossing in **1i** due to steric conditions in the interior of the macrocycle. The absorption spectra of these porphyrins were also examined using the results from B3LYP/6-31G(d)//B3LYP/3-21G(d) calculations and interpreted using the four electron four orbital model.

Introduction

Investigations into the optical properties and photophysical behavior of porphyrins continue to attract much interest. Porphyrin photochemistry provides insight into the dynamics of related biomolecules, such as the photosynthetic reaction centers in purple bacteria and green plants and heme-based metalloproteins such as hemoglobin and myoglobin. Much of this work has recently been focused on free-base and metalloporphyrin assemblies for light-harvesting purposes,[1] porphyrin-containing mimics of the photosynthetic reaction center,[2] and electronic devices.[3] Although the impetus for research in this area is the creation of molecular candidates for understanding and duplicating the photoinduced processes involved in solar energy conversion, these systems also help advance our knowledge of fundamental photochemical processes such as electronic and vibrational relaxation,[4] energy transfer,[5] and solvent dynamics.[6]

Although the photophysics of free-base and metalloporphyrins has been extensively investigated,[7] similar experiments have yet to be carried out on many of the isomers and analogues of porphyrins. These analogues and isomers, however, can also provide much data on the photodynamics of natural porphyrin-related chromophores. One such class of macrocycles is the N-confused porphyrins, isomers of porphyrins with one of the pyrrolic nitrogens facing outside the macrocycle and a C−H group oriented inward toward the core. These macrocycles, while differing from the parent tetrapyrrole by the inversion of only two atoms, have quite different physical and chemical properties. With regard to electronic structure, N-confused porphyrins have decreased symmetry and reduced aromaticity relative to the parent macrocycle.[8] These attributes make N-confused porphyrins similar to both chlorophylls and porphyrins, and may be potential models for natural light-harvesting systems. Another notable aspect of N-confused porphyrins is that, although their electronic structure is significantly altered, the macrocycle is only slightly more sterically demanding (for the internally protonated tautomer only) than normal porphyrins. Thus, metalated systems may help illuminate the reasons behind the biological selection of porphyrin as the tetrapyrrole of choice in metalloenzymes. Part of the impetus for this work was to determine the potential for using N-confused porphyrins as building blocks in artificial photosynthetic macromolecules and dendrimers.[9]

In this work, we present the first photophysical study of two of the tautomers (**1e** and **1i**) of 5,10,15,20-tetraphenyl N-confused porphyrin free-base. The predominance of a particular N-confused porphyrin tautomer is highly dependent upon solvent, with the "externally protonated" tautomer (**1e**) favored in highly polar solvents such as DMF, and the "internally protonated" form (**1i**) preferred in aromatic and halogenated solvents. Herein, we report the fluorescence spectra, fluorescence quantum yields, and fluorescence lifetimes of both tautomers in solution. In addition, we have carried out density functional (DFT) calculations to probe the electronic structure of both tautomers, both to understand further the nature of excitation and emission in these macrocycles and to draw analogies to naturally occurring tetrapyrroles such as chlorin and chlorophylls.

Experimental Section

General Methods. Absorption experiments were carried out on a Hitachi 3100 single monochromator UV−vis spectrophotometer. The Q-band absorption assignments were made by analogy to normal porphyrin Q-band absorptions. Steady-state fluorescence measurements were run on a ISA Jobin Yvon-

* To whom correspondence should be addressed. E-mail: ziegler@chemistry.uakron.edu. E-mail: dam@chemistry.uakron.edu.

[†] Department of Chemistry, The University of Akron.

[‡] Department of Chemistry and The Center for Laser and Optical Spectroscopy, The University of Akron.

10.1021/jp025569w CCC: $22.00
Published on Web 06/07/2002

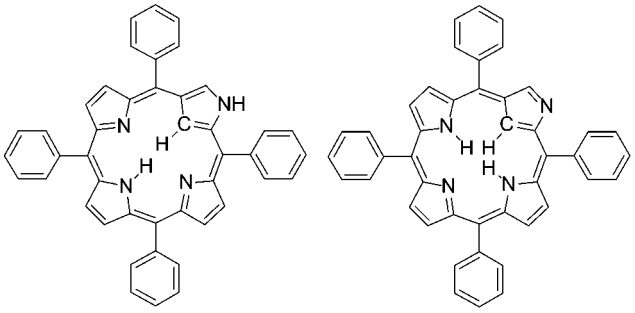

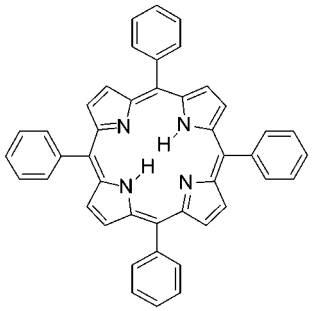

SPEX Fluorolog 3−22 fluorometer equipped with dual input and output monochromators. Fluorescence spectra were collected using argon-saturated solutions by exciting at the Soret maxima in S/R mode to correct for changes in the lamp output intensity. Quantum yield measurements were made relative to H_2TPP.[10] All solvents used for spectroscopic measurements were spectrophotometric grade and were used as received, except chloroform, which was passed through a plug of silica gel to remove HCl.

Synthesis. 2-Aza-21-carba-5,10,15,20-tetraphenyl porphyrin (H_2NCTPP, **1**) was prepared by using the synthetic protocol developed by Geier et al.[11] Additional purification of **1** was accomplished by passage through an additional basic alumina column using dichloromethane and hexanes as the eluents.

Computational Methods. Geometry optimizations were performed using Becke's gradient corrected three-parameter[12] exchange functional with the correlation functional of Lee, Yang, and Parr[13] (B3LYP[14]). The 3-21G(d) basis set was used for all geometry optimizations. Single-point energies were computed at the B3LYP/6-31G(d) level using both computed (B3LYP/6-31G(d)//B3LYP/3-21G(d)) and single crystal (B3LYP/6-31G(d)//single crystal) geometries. Only the B3LYP/6-31G(d)//B3LYP/3-21G(d) information is reported here due to divergence from orthogonality of the phenyl rings in the porphyrin structures caused by crystal packing forces. Structural details are provided in the Supporting Information. All calculations were performed within Gaussian 98.[15] Molecular orbitals were visualized using MacMolPlt[16] and calculated with MacGAMESS.[17] The electronic structure of **1** is interpreted in the context of Gouterman's four-electron four-orbital model.[7] The symmetries of the four frontier orbitals are slightly distorted from those found in porphyrins because of the inverted ring but are nonetheless close enough to use the conventional nomenclature to describe the N-confused porphyrin orbitals. Thus, the LUMO and LUMO+1 orbitals are analogous to the e_g orbitals in normal porphyrins (and are so named), and the HOMO and HOMO-1 orbitals are a_{2u} and a_{1u}, respectively. For convenience, we refer to the inverted pyrrole ring as the "A ring" and the other pyrrole rings as the B through D rings.

Time-Resolved Fluorescence Measurements. All solvents used for spectroscopic measurements were either spectrophotometric or HPLC-grade. Time-resolved fluorescence experiments were performed using the time-correlated single-photon counting (TCSPC) technique. The experimental apparatus used in this work has been described previously[9] and utilizes the pulses from a Coherent 702 dye laser pumped by the 532 nm output of a Coherent Antares 76-s CW mode-locked Nd:YAG laser. The fluorescence signals were detected at 55° with an emission polarizer and depolarizer, using a Hamamatsu R3809U-51 red-sensitive microchannel plate detector. Data collection and analysis were accomplished with an Edinburgh Instruments data collection system. The time-resolution of this system is estimated at ∼7−9 ps after reconvolution. H_2TPP was excited with 590 nm light and its decay profile monitored at 655 nm. N-confused porphyrins **1e** and **1i** were excited with 590 nm light and the decay profiles monitored at the emission maxima. All experiments were run with argon-saturated solutions. TCSPC measurements on H_2TPP show a clean single-component decay, whereas the analogous N-confused porphyrin in either solvent was best fit to a multiexponential decay using the Marquardt algorithm.[18] All measurements were fit such that values of $\chi^2 < 1.20$ were obtained. Error limits in these measurements are typically ±10%.

Results and Discussion

Computational Results. Detailed molecular orbital calculations (B3LYP/6-31G(d)) probing the metal-complexing ability of N-confused porphines such as **2e** and **2i** were first reported by Szterenberg and Latos-Grazynski.[8a] The relative energies of tautomers **2e** and **2i**, as well as several structural isomers, were later reported by Ghosh and co-workers,[8b,8c] who also commented extensively on the relative stabilities of **2e** and **2i**. Their results indicated an energetic preference for **2i** that results from the presence of the aromatic [18]annulene ring path also present in porphyrins. Tautomer **2e** lacks such a delocalizing pathway, resulting in a highly conjugated but nonaromatic macrocycle. However, a surprisingly small energetic difference was observed between the two tautomers (∼3.4−5.7 kcal mol^{-1}), which was attributed to the destabilizing effects of the extra hydrogen inside the macrocycle in **2i**, which counteracts most of the stabilization resulting from resonance. Both sets of calculations predict a substantial energetic difference between **2i** and porphine (∼21.5 kcal mol^{-1} in Latos-Grazynski's calculations[8a] and 17.7 kcal mol^{-1} as reported by Ghosh[8b]). Neither group evaluated the absorption spectra of the N-confused porphines in terms of Gouterman's four-electron four-orbital model. Calculations at the semiempirical level (AM1, PM3) were performed by Zandler and D'Souza[8c] examining the electronic structure of the theoretical zinc and magnesium complexes of **2** (i.e., **M-2**). In these calculations, a reasonable qualitative agreement with the four-electron four-orbital model was found, although the HOMO-1 orbital (analogous to the porphyrin a_{2u} orbital) differed significantly from that of a similarly metalated porphine.

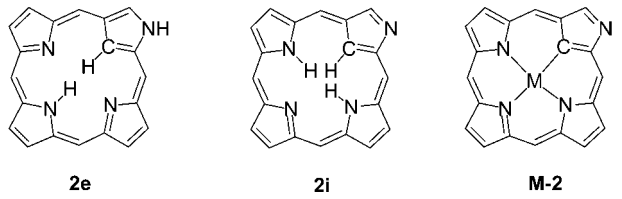

To provide reliable orbital energies and electronic structures for **1e** and **1i**, as well as to help elucidate the factors that

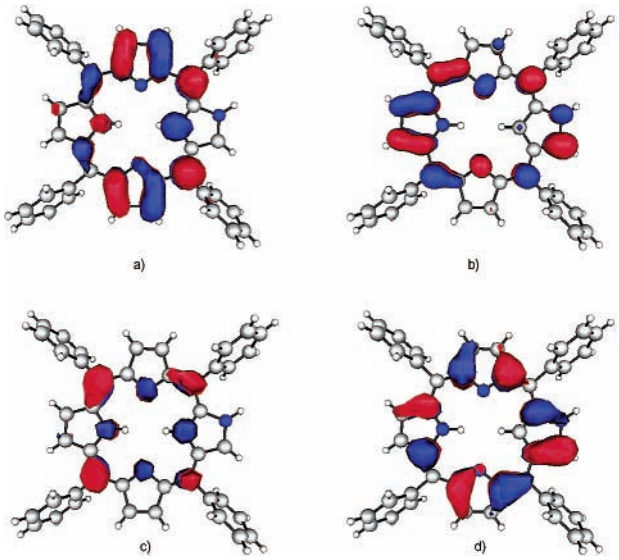

Figure 1. Plots of the LUMO+1 (a), LUMO (b), HOMO (c), and HOMO-1 (d) molecular orbitals for N-confused porphyrin **1e**.

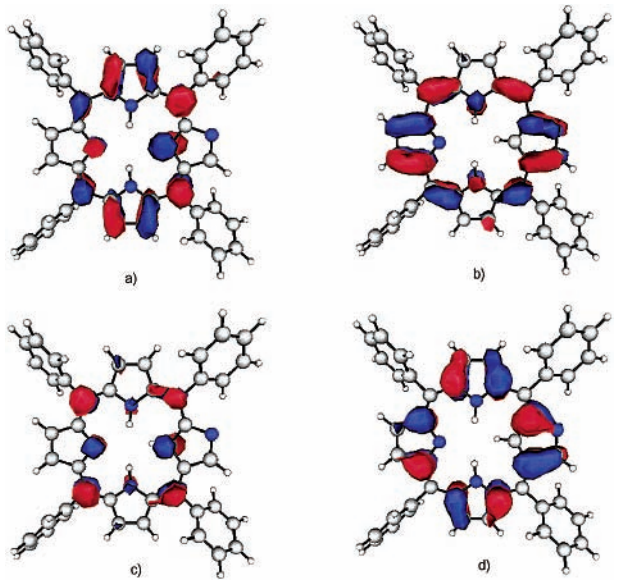

Figure 2. Plots of the LUMO+1 (a), LUMO (b), HOMO (c), and HOMO-1 (d) molecular orbitals for N-confused porphyrin **1i**.

contribute to the photophysical similarities and differences with H_2TPP and tetraphenylchlorin (H_2TPChl), we calculated the geometries and ground-state electronic structures of **1e**, **1i**, H_2-TPP, and H_2TPChl at the B3LYP/6-31G(d)//B3LYP/3-21G(d) level. The computed structures for **1e** and **1i** agree well with crystal structures.[19,20] The energetic differences (Table 1) between **1e**, **1i**, and H_2TPP are comparable to those found for the unsubstituted porphyrins, with **1i** more stable than **1e** by ~5.5 kcal mol^{-1} at the B3LYP/6-31G(d)//B3LYP/3-21G(d) level. Plots of the two highest occupied and the two lowest unoccupied MOs for **1e**, **1i**, H_2TPChl, and H_2TPP are shown in Figures 1−4. The MOs for both **1e** and **1i** are ring-based and qualitatively similar to those predicted by Gouterman's four-electron four-orbital model.[7]

The lowest two unoccupied orbitals of **1e** (Figure 1a,b) are both of e_g symmetry and are qualitatively similar to those of H_2TPP and H_2TPChl. Because of the decrease in symmetry in the ring of **1e**, the e_g orbitals are nondegenerate and separated in energy at the B3LYP/6-31G(d)//B3LYP/3-21G(d) level by ~0.6130 eV (Table 2). The LUMO orbital is stabilized relative

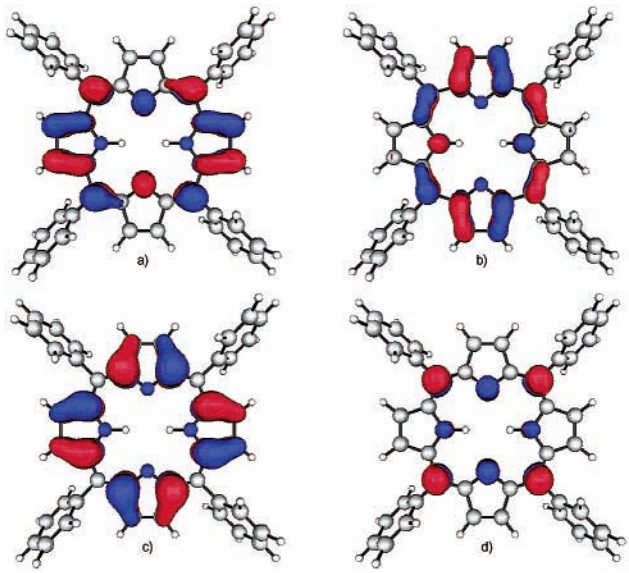

Figure 3. Plots of the LUMO+1 (a), LUMO (b), HOMO (c), and HOMO-1 (d) molecular orbitals for tetraphenylporphyrin (H_2TPP).

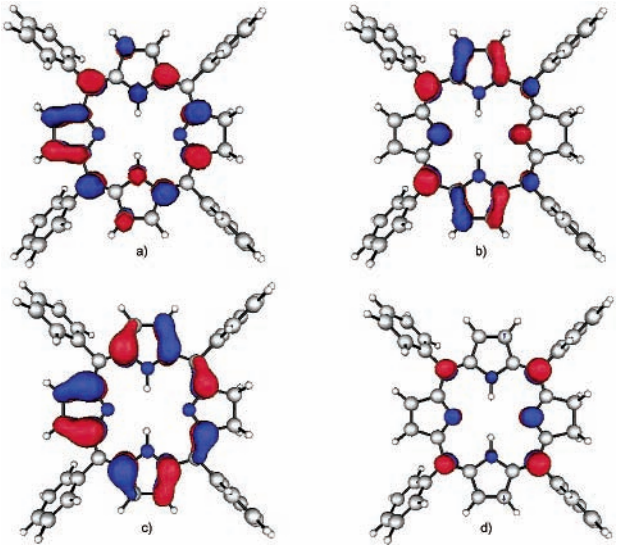

Figure 4. Plots of the LUMO+1 (a), LUMO (b), HOMO (c), and HOMO-1 (d) molecular orbitals for tetraphenylchlorin (H_2TPChl).

TABLE 1: Relative Energies (kcal mol^{-1}) of N-Confused Porphyrins 1e and 1i and Tetraphenylporphyrin (H_2TPP) at the B3LYP/3-21G(d) and B3LYP/6-31G(d)//B3LYP/3-21G(d) Levels of Theory

compound	B3LYP/3-21G(d)	B3LYP/6-31G(d)// B3LYP/3-21G(d)
1e	20.4	18.7
1i	17.1	13.2
H_2TPP	0.00	0.00

to the nearly degenerate e_g orbitals in H_2TPP, and relative to the LUMO in H_2TPChl. Unlike the two highest occupied orbitals in H_2TPP and H_2TPChl that have a_{1u} (HOMO) and a_{2u} (HOMO-1) symmetry, the HOMO in **1e** has a_{2u} symmetry, and the HOMO-1 is in a_{1u} symmetry. The energy separation between these orbitals is 0.7156 eV at the B3LYP/6-31G(d)//B3LYP/3-21G(d) level. This energy difference is substantially larger than that found in either H_2TPP (0.2220 eV) or H_2TPChl (0.1412 eV). The difference in energy arises from destabilization of the a_{2u} HOMO of **1e**, which is 0.4528 and 0.3034 eV higher in energy than the HOMO of H_2TPP and H_2TPChl, respectively. The result of destabilization of the HOMO is a smaller HOMO−

TABLE 2: Computational Results for N-Confused Porphyrins 1e and 1i, Tetraphenylporphyrin (H_2TPP) and Tetraphenylchlorin (H_2TPChl)

method	orbital	**1e**	**1i**	H_2TPP	H_2TPChl
B3LYP/3-21G(d)	LUMO+1	−0.06589 (−1.7930 eV)	−0.08592 (−2.3380 eV)	−0.08083 (−2.1995 eV)	−0.06146 (−1.6724 eV)
	LUMO	−0.08803 (−2.3954 eV)	−0.08918 (−2.4267 eV)	−0.08107 (−2.2060 eV)	−0.08014 (−2.1807 eV)
	HOMO	−0.16574 (−4.5100 eV)	−0.17951 (−4.8847 eV)	−0.18278 (−4.9737 eV)	−0.18079 (−4.9195 eV)
	HOMO-1	−0.19673 (−5.3533 eV)	−0.20209 (−5.4991 eV)	−0.19561 (−5.3228 eV)	−0.18204 (−4.9536 eV)
B3LYP/6-31G(d)// B3LYP/3-21G(d)	LUMO+1	−0.06446 (−1.7540 eV)	−0.08401 (−2.2860 eV)	−0.07938 (−2.1600 eV)	−0.06051 (−1.6466 eV)
	LUMO	−0.08697 (−2.3670 eV)	−0.08702 (−2.3679 eV)	−0.08015 (−2.1810 eV)	−0.08007 (−2.1788 eV)
	HOMO	−0.16497 (−4.4891 eV)	−0.17696 (−4.8153 eV)	−0.18161 (−4.9419 eV)	−0.17612 (−4.7925 eV)
	HOMO-1	−0.19127 (−5.2047 eV)	−0.19590 (−5.3307 eV)	−0.18977 (−5.1639 eV)	−0.18131 (−4.9337 eV)

TABLE 3: Summary of Absorption Data for N-Confused Porphyrin Tautomers 1e and 1i, Porphyrin H_2TPP, and Chlorin H_2TPChl

compound	solvent	Soret (nm) ($\epsilon \times 10^4$ M^{-1} cm^{-1})	Q-bands (nm) ($\epsilon \times 10^3$ M^{-1} cm^{-1})			
1i	$CHCl_3$	438 (15.9)	539 (7.8)	580 (10.8)	665 (2.7)	724 (10.4)
1e	DMAc	442 (11.9)	550 (2)	595 (6.1)	644 (9.5)	699 (12.4)
H_2TPP[a]	$CHCl_3$	419 (41.1)	515 (17.3)	550 (8.1)	590 (6.4)	645 (6.2)
H_2TPP[b]	DMAc	417 (48.5)	513 (20.8)	548 (9.67)	591 (6.69)	646 (6.05)
H_2TPChl[c]	C_6H_6	419 (1.85)	520 (15)	545 (11)	595 (5.5)	650 (42)

[a] Taken from Dudic, M.; Lhoták, P.; Král, V.; Long, K.; Stibor, I. *Tetrahedron Lett.* **1999**, *40*, 5949−5952. [b] Taken from Datta-Gupta, N.; Malakar, D.; Rice, L.; Rivers, S. *J. Heterocycl. Chem.* **1987**, *24*, 629−632. [c] Taken from Dorough, G. D.; Huennekens, F. M. *J. Am. Chem. Soc.* **1952**, *74*, 3974.

LUMO gap of (2.1221 eV) than is found for H_2TPP (2.7609 eV) or H_2TPChl (2.6137 eV). It is clear from this discussion that there are significant electronic changes imparted upon the macrocycle in **1e** by inversion of the pyrrole ring.

The structure of **1i** is significantly distorted from planarity by the presence of the extra hydrogen inside the macrocycle, resulting in the internal C−H bond in the A ring having a dihedral angle of ∼21° to the plane of the macrocycle. The shapes of the orbitals in **1i** are clearly affected by this deformation of the inverted pyrrole ring, and are substantially less symmetric than those of **1e** (Figure 2). As with **1e**, however, the HOMO and HOMO-1 orbitals in **1i** are reversed in energy relative to H_2TPP and have a_{2u} symmetry (HOMO) and a_{1u} symmetry (HOMO-1). The energies of the MOs of **1i** are surprisingly similar to those found for H_2TPP and H_2TPChl at the B3LYP/6-31G(d)//B3LYP/3-21G(d) level of theory (Table 2). The unoccupied orbitals are nearly degenerate and are of e_g symmetry (−2.3380 and −2.4267 eV), whereas the HOMO−LUMO gap is 2.4580 eV (compared to 2.7609 eV for H_2TPP). The parity of the orbital energies no doubt accounts for the similarities in the absorption spectra of **1i** and H_2TPChl. To summarize, the electronic structure of **1i** is surprisingly less affected by inversion of the pyrrole ring than is **1e**.

Steady State Absorption. Absorption spectra (Figure 5, Table 3) obtained for **1** display striking differences compared to H_2TPP and are highly solvent dependent. The absorption spectra recorded here are in good agreement with those reported by Furuta et al.,[20] who interpreted the differences in the observed spectra to arise from two tautomers (i.e., **1e** and **1i**). In a polar solvent such as dimethylacetamide (DMAc), the externally protonated form (**1e**) is more stable, presumably because of either hydrogen-bonding or dipole−dipole interactions of the exocyclic N−H bond with solvent, whereas a less polar solvent such as $CHCl_3$ tends to favor the internally protonated form, **1i**. In DMAc, the Soret band for **1e** is significantly red-shifted (441 nm) relative to the Soret band of H_2TPP (419 nm). Three

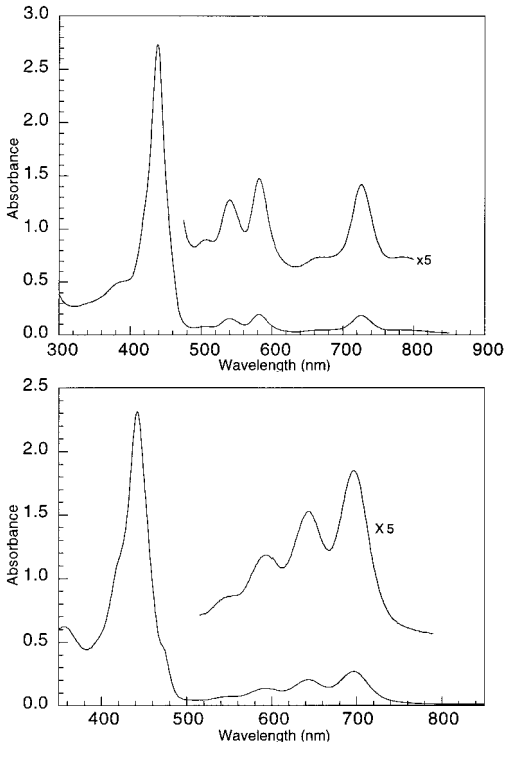

Figure 5. Absorption spectra of **1i** (chloroform, top) and **1e** (dimethylacetamide, bottom).

Q-band absorptions of increasing intensity are found at 695, 642, and 592 nm, along with a smaller shoulder at 550 nm. These absorptions are analogous to the $Q_x(0,0)$, $Q_x(1,0)$, $Q_y(0,0)$, and $Q_y(1,0)$ transitions, respectively, in H_2TPP. Similar to the red-shift in the Soret band, these bands are ∼37−50 nm lower in energy than the corresponding absorptions in H_2TPP. Unlike H_2TPP, however, the intensities of these bands increase

TABLE 4: Summary of Fluorescence Data for N-Confused Porphyrin Tautomers 1e and 1i, Porphyrin H_2TPP, and Chlorin H_2TPChl

compound	solvent	fluorescence maxima (nm)[a]	Φ_{Fl}[b]	τ_1[c] (ns)	τ_2[c] (ns)	τ_3[c] (ns)	Stokes shift (cm^{-1})
1i	$CHCl_3$	744/815	0.00156	1.60 (95%)			371
1e	DMAc	713/783	0.03648	1.98 (87%)	0.68 (9%)	0.025 (4%)	281
H_2TPP	$CHCl_3$	651/715	0.11	9.25			143
H_2TPP	DMAc	650/715	0.11	12.2			95
H_2TPChl	C_6H_6	660/730[d]					233

[a] Excited at the Soret bands to avoid aggregation due to concentration effects. [b] Relative to the fluorescence of H_2TPP. Quantum yields were calculated using standard methods. [c] Fluorescence lifetimes were determined by exciting argon-purged and stirred solutions of the respective porphyrins with the 570 nm output of a Coherent 700 dye laser pumped by the 532 nm output of a Coherent Antares 76-s CW mode-locked Nd:YAG laser. Emission was detected at the appropriate wavelength and measured at 55° with an emission polarizer and depolarizer, using a Hamamatsu R3809U-51 multichannel plate detector. Values in parentheses are the relative contribution from each component. [d] Taken from ref 22b.

slightly with decreasing energy, with the lowest-energy absorption being most intense. A high-energy band occurring at 381 nm is attributed to the N-band absorption.[21]

In $CHCl_3$, the Soret band for **1i** is similarly red-shifted (438 nm). Three pronounced Q-band absorptions are observed in $CHCl_3$, at 539, 580, and 724 nm, with two smaller absorptions at 504 and 665 nm. An increase in the intensities of the Q-band absorptions is also observed in **1i** that corresponds with a decrease in the absorption band energy. We assign the absorption at 724 nm to the $Q_x(0,0)$ band and the small absorption at 665 nm to the $Q_x(1,0)$ band. The absorptions at 539 and 580 nm are attributed to the $Q_y(1,0)$ and $Q_y(0,0)$ bands, respectively. Two weak absorptions are observed at 353 and 504 nm, with the former being attributed to the N band. The intensity profile of the Q-band region, particularly that of the low energy absorption at 724 nm for **1i**, is reminiscent of the absorption spectra of reduced porphyrins (i.e., hydrogenated at one of the pyrrole rings) such as chlorins and chlorophylls *a* and *b*.

The decrease in symmetry in the macrocycle induced by the inversion of one of the pyrrole rings, and the anticipated change in the electronic structure, begs a comparison with reduced porphyrins such as chlorin and chlorophyll *b*. In reduced porphyrins, the four-electron four-orbital model is modified to reflect the loss of degeneracy of the unoccupied e_g and occupied a_{1u} and a_{2u} orbitals. The absorption spectrum of H_2TPChl[22] in benzene is quite similar in its intensity pattern to **1i** (Table 3). A broad Soret band occurs at ~419 nm, whereas the Q-band region is dominated by the intense $Q_x(0,0)$ band at 650 nm, a very weak $Q_x(1,0)$ absorption at 595 nm, and intense $Q_y(0,0)$ and $Q_y(1,0)$ bands at 545 and ~520 nm, respectively. Although the bands for H_2TPChl are not substantially shifted from those of H_2TPP, the intensities of the absorptions are significantly different (Table 3). Using the four-electron four-orbital model, Weiss[23] has ascribed the change in the intensity pattern in the Q-band region of H_2TPChl to the low energy $Q_x(0,0)$ band becoming weakly allowed from the decrease in symmetry resulting from the loss of degeneracy in of the e_g orbitals. A comparison of the relative intensities of the Q bands in H_2TPChl and **1i** shows the ratio $Q_x(0,0)/Q_x(1,0)$ to be 7.6 for H_2TPChl and 3.9 for **1i**, which contrasts the same ratio for H_2TPP (0.97 in $CHCl_3$).[24] The ratio $Q_y(0,0)/Q_y(1,0)$ is also similar for these two compounds, where values of 0.73 (H_2TPChl) and 0.64 (**1i**) are found.

The absorption spectrum for **1e**, despite the significant red-shift in both the Soret and Q-band regions, resembles the spectrum of H_2TPP more closely than the spectrum of H_2TPChl. The Q-band oscillator strengths increase with decreasing energy in a regular fashion, so that the $Q_x(0,0)$ band is the most intense and the $Q_y(1,0)$ band is the weakest. Integration of the $Q_x(0,0)$ bands in **1i** and H_2TPP indicates an ~53% increase in the ground state ↔ Q-state excited-state transition in **1i** relative to H_2TPP. A similar analysis for **1e** showed a ~64% increase in the ground state ↔ Q-state excited-state transition for **1e** (relative to H_2TPP). These results are consistent with a decrease in the forbidden nature of the $S_0 \rightarrow S_1$ transitions for **1i** and **1e** that are promoted by the degeneracy of the e_g orbitals.

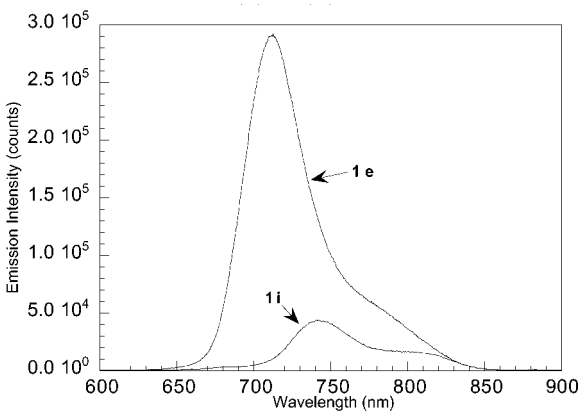

Figure 6. Emission spectra of **1i** (chloroform) and **1e** (dimethylacetamide).

Fluorescence Experiments. Steady-state fluorescence measurements reveal a large $Q_x(0,0)$ emission band for **1i** (in $CHCl_3$) at 744 nm, and a small low energy $Q_x(0,1)$ shoulder at 815 nm (Table 4, Figure 6). In DMAc, the predominant $Q_x(0,0)$ emission for **1e** is observed at 713 nm, with a corresponding $Q_x(0,1)$ shoulder at 783 nm (Table 4, Figure 6). The fluorescence spectra are significantly red-shifted from H_2TPP (651 and 715 nm in either solvent) and H_2TPChl (660 and 730 nm in benzene).[22b,25] These shifts are consistent with the red-shifts observed in the absorption spectra (Table 3). The ratio of the $Q_x(0,0)$ and $Q_x(0,1)$ emission bands, similar to that of the $Q_x(0,0)$ and $Q_x(1,0)$ absorption bands, is increased relative to H_2TPP. Again, these changes are attributed to changes in the ground state ↔ Q-state excited-state transitions for **1e** and **1i**.[26] The natural radiative rates for these N-confused porphyrins (**1i**: ~$(70\ ns)^{-1}$ and **1e**: ~$(50\ ns)^{-1}$) are therefore substantially reduced from that for H_2TPP (~$(120\ ns)^{-1}$).[7]

Fluorescence lifetimes (Table 4) for **1i** and **1e** were determined using the time-correlated single-photon counting (TC-SPC) technique. The lifetime of N-confused porphyrin **1i** in $CHCl_3$ is 1.60 ns, approximately six times shorter than that of H_2TPP (~9.25 ns) in the same solvent. In DMAc, the lifetime is 1.98 ns and is also significantly shorter than that of H_2TPP in the same solvent (12.2 ns). Two very short-lived components to the decay trace were also observed in DMAc (680 ps, 9%, and 25 ps, 4%).

The quantum yields of fluorescence (Table 4, Φ_{Fl}) for **1e** and **1i** are significantly smaller than Φ_{Fl} for H_2TPP (Φ_{Fl} =

0.11).[10] The large difference most likely results from the reduced radiative (fluorescence) rate of the N-confused porphyrins. Interestingly, the quantum yield of **1e** ($\Phi_{Fl} = 0.036$) is larger by a factor of more than twenty than that of **1i** ($\Phi_{Fl} = 0.0016$), despite the similarities in the fluorescence lifetime values. The changes in fluorescence quantum yield can be attributed in part to the different natural radiative rates between the two porphyrins ($\sim(70\ ns)^{-1}$ vs $\sim(50\ ns)^{-1}$).[10] However, the bulk of the change in quantum yield probably results from differences in the internal conversion or intersystem crossing rate constants between the two N-confused porphyrins. The macrocycle in **1i** has three hydrogens in the core, promoting ring deformation that can provide a ready mechanism for efficient internal conversion or intersystem crossing. We feel differences between these two nonradiative decay pathways are responsible for making **1i** so much less emissive than **1e**.

Conclusions

We have studied the photophysical properties of N-confused porphyrins from the joint perspectives of probing their potential usefulness in molecular photonic devices, as well as exploring the biological choice of chlorins and chlorophylls as light-harvesting macrocycles in natural photosynthetic systems. It is important to reiterate the similarities and differences among the N-confused porphyrin tautomers, porphyrins, and reduced porphyrins. The absorption spectra of N-confused porphyrins and regular porphyrins are quite different, probably because of a decrease in symmetry of the N-confused porphyrin ring. The decrease in symmetry was shown by density functional theory to result in a loss in degeneracy of the lowest pair of unoccupied orbitals which shifts the energy of both Soret and Q-band absorptions of the N-confused porphyrins to lower energies and also makes the Q-band absorptions more allowed than the analogous transitions in H_2TPP. In addition, the fluorescence quantum yields and fluorescence lifetimes of both N-confused tautomers are significantly smaller than those of H_2TPP. The absorption characteristics of N-confused porphyrins are quite similar to reduced porphyrins, a similarity that is attributed to the aforementioned reduction in symmetry. Interestingly, N-confused porphyrins also have greatly reduced fluorescent lifetimes and fluorescence quantum yields relative to chlorins and chlorophylls. Goutermann's four electron four orbital model provides insight into the similarities in the absorption spectra between N-confused porphyrins and reduced porphyrins. This simple model, however, does not sufficiently explain the differences in the observed decay kinetics of the excited singlet states of the N-confused porphyrins. We propose that the nonplanar structure for **1i**, resulting from the steric congestion of three hydrogens inside the porphyrin core, leads to an increase in either (or both) the rate constants for internal conversion (k_{IC}) or intersystem crossing (k_{ISC}). Further investigations into the factors that result in the reduced fluorescence quantum yields and fluorescence lifetimes in the N-confused porphyrins should provide a deeper understanding into the highly efficient light harvesting macrocycles found in nature, and in doing so afford insight into how to reproduce this chemistry with designed systems.

The short-lived excited states observed for **1i** and **1e** (relative to H_2TPP) do not rule out their potential use as polarity dependent switching devices or as model compounds for processes related to artificial photosynthesis. Indeed, these macrocycles possess superior absorption properties in the visible region of the absorption spectrum relative to regular porphyrins and have fluorescence lifetimes similar to commonly used metalloporphyrins such as ZnTPP. Because of the differences in electronic structure and planarity, the two tautomers may differ in how they engage in energy and/or electron transfer to acceptor molecules. Because the nature of the protonation in N-confused porphyrins is seemingly governed by solvation, these processes might be readily controlled. We are currently extending our investigations into the photophysical properties of N-confused porphyrin/quinone donor/acceptor dyads to explore electron-transfer processes in these molecules.[27]

Acknowledgment. D.A.M. gratefully acknowledges the support of the National Science Foundation in the form of a CAREER Award (NSF-9875489) and a CRIF Grant (NSF-9816260), the Ohio Board of Regents, and The University of Akron for a Faculty Research Grant (FRG-07368). C.J.Z. acknowledges The University of Akron for a Faculty Research Grant (FRG-1524). We also thank Professor Edward C. Lim for the use of his picosecond laser and helpful discussions.

Supporting Information Available: Cartesian coordinates and energies for all computed structures (**1e**, **1i**, H_2TPP, and H_2TPChl). This material is available free of charge via the Internet at http://pubs.acs.org.

References and Notes

(1) (a) Lammi, R. K.; Ambroise, A.; Balasubramian, T.; Wagner, R. W.; Bocian, D. F.; Holten, D.; Lindsey, J. S. *J. Am. Chem. Soc.* **2000**, *122*, 7579−7591. (b) Rao, P. D.; Dhanalekshmi, S.; Littler, B. J.; Lindsey, J. S. *J. Org. Chem.* **2000**, *65*, 7323−7344. (c) Li, J.; Ambroise, A.; Yang, S. I.; Diers, J. R.; Seth, J.; Wack, C. R.; Bocian, D. F.; Holten, D.; Lindsey, J. S. *J. Am. Chem. Soc.* **1999**, *121*, 8927−8940. (d) Li, J.; Diers, J. R.; Seth, J.; Yang, S. I.; Bocian, D. F.; Holten, D.; Lindsey, J. S. *J. Org. Chem.* **1999**, *64*, 9090−9100. (e) Yang, S. I.; Seth, J.; Balasubramanian, T.; Kim, D.; Lindsey, J. S.; Holten, D.; Bocian, D. F. *J. Am. Chem. Soc.* **1999**, *121*, 4008−4018. (f) Shediac, R.; Gray, M. H. B.; Uyeda, H. T.; Johnson, R. C.; Hupp, J. T.; Angiolillo, P. J.; Therien, M. J. *J. Am. Chem. Soc.* **2000**, *122*, 7017−7033. (g) Iovine, P. M.; Kellett, M. A.; Redmore, N. P.; Therien, M. J. *J. Am. Chem. Soc.* **2000**, *122*, 8717−8727. (h) Kumble, R.; Palese, S.; Lin, V. S.-Y.; Therien, M. J.; Hochstrasser, R. M. *J. Am. Chem. Soc.* **1998**, *120*, 11489−11498. (i) Hyslop, A. G.; Therien, M. J. *Inorg. Chim. Acta* **1998**, *275*−*276*, 427−434. (j) Priyadarshy, S.; Therien, M. J.; Beratan, D. N. *J. Am. Chem. Soc.* **1996**, *118*, 1497−503.

(2) (a) Gust, D.; Moore, T. A. In *The Porphyrin Handbook: Electron Transfer*; Kadish, K. M., Smith, K. M., Guilard, R., Eds.; Academic Press: San Diego, 2000; Vol. 8. (b) Kuciauskaas, D.; Liddell, P. A.; Lin, S.; Johnson, T. E.; Weghorn, S. J.; Lindsey, J. S.; Moore, A. L.; Moore, T. A.; Gust, D. *J. Am. Chem. Soc.* **1999**, *121*, 8604−8614. (c) Steinberg-Yfrach, G.; Rigaud, J.-L.; Durantini, E. N.; Moore, A. L.; Gust, D.; Moore, T. A. *Nature* (*London*) **1998**, *392*, 479−482 (d) Steinberg-Yfrach, G.; Liddell, P. A.; Hung, S.-C.; Moore, A. L.; Gust, D.; Moore, T. A. *Nature* (*London*) **1997**, *385*, 239−241. (e) Gust, D.; Moore, T. A.; Moore, A. L. *Pure Appl. Chem.* **1998**, *70*, 2189−2200. (f) Maniga, N. I.; Sumida, J. P.; Stone, S.; Moore, A. L.; Moore, T. A.; Gust, D. *J. Porphyrins Phthalocyanines* **1999**, *3*, 32−44. (g) Sumida, J. P.; Liddell, P. A.; Lin, S.; Macpherson, A. N.; Seely, G. R.; Moore, A. L.; Moore, T. A.; Gust, D. *J. Phys. Chem. A* **1998**, *102*, 5512−5519.

(3) (a) Levanon, H.; Galili, T.; Regev, A.; Wiederrecht, G. P.; Svec, W. A.; Wasielewski, M. R. *J. Am. Chem. Soc.* **1998**, *120*, 6366−6373. (b) Gaines, G. L., III.; O'Neil, M. P.; Svec, W. A.; Niemczyk, M. P.; Wasielewski, M. R. *J. Am. Chem. Soc.* **1991**, *113*, 719−721. (c) Wasielewski, M. R.; Niemczyk, M. P.; Svec, W. A.; Pewitt, E. B. *J. Am. Chem. Soc.* **1985**, *107*, 5562−5563. (d) Wasielewski, M. R.; Niemczyk, M. P.; Svec, W. A.; Pewitt, E. B. *J. Am. Chem. Soc.* **1985**, *107*, 1080−1082. (e) Wasielewski, M. R.; Niemczyk, M. P. *J. Am. Chem. Soc.* **1984**, *106*, 5043−5045.

(4) (a) Retsek, J. L.; Gentemann, S.; Medforth, C. J.; Smith, K. M.; Chirvony, V. S.; Fajer, J.; Holten, D. *J. Phys. Chem. B* **2000**, *104*, 6690−6693. (b) Mataga, N.; Shibata, Y.; Chosrowjan, H.; Yoshida, N.; Osuka, A. *J. Phys. Chem. B* **2000**, *104*, 4001−4004. (c) Akimoto, S.; Yamazaki, T.; Yamazaki, I.; Osuka, A. *Chem. Phys. Lett.* **1999**, *309*, 177−182.

(5) (a) Balzani, V.; Ceroni, P.; Juris, A.; Venturi, M.; Campagna, S.; Puntoriero, F.; Serroni, S. *Coord. Chem. Rev.* **2001**, *219*, 545−572. (b) Nakano, A.; Osuka, A.; Yamazaki, T.; Nishimura, Y.; Akimoto, S.; Yamazaki, I.; Itaya, A.; Murakami, M.; Miyasaka, H. *Chem.-Eur. J.* **2001**, *7*, 3134−3151. (c) Lammi, R. K.; Ambroise, A.; Balasubramanian, T.;

Wagner, R. W.; Bocian, D. F.; Holten, D.; Lindsey, J. S. *J. Am. Chem. Soc.* **2000**, *122*, 7579−7591. (d) Ward, M. D. *Chem. Soc. Rev.* **1997**, *26*, 365−375.

(6) (a) Kilsa, K.; Kajanus, J.; Macpherson, A. N.; Martensson, J.; Albinsson, B. *J. Am. Chem. Soc.* **2001**, *123*, 3069−3080. (b) Macpherson, A. N.; Liddell, P. A.; Lin, S.; Noss, L.; Seely, G. R.; Degraziano, J. M.; Moore, A. L.; Moore, T. A.; Gust, D. *J. Am. Chem. Soc.* **1995**, *117*, 7202−7212. (c) Wiederrecht, G. P.; Watanabe, S.; Wasielewski, M. R. *Chem. Phys.* **1993**, *176*, 601−614.

(7) Gouterman, M. J. In *The Porphyrins*; Dolphin, D., Ed.; Academic Press: New York, 1978; Vol. III, pp 1−165. Seybold, P. G.; Gouterman, M. *J. Mol. Spectrosc.* **1969**, *31*, 1−13.

(8) (a) Parusel, A. B. J.; Ghosh, A. *J. Phys. Chem. A* **2000**, *104*, 2504−2507. (b) Ghosh, A.; Wondimagegn, T.; Nilsen, H. *J. Phys. Chem. B* **1998**, *102*, 10459−10467. (c) Zandler, M. E.; D'Souza, F. *J. Mol. Struct. (THEOCHEM)* **1997**, *401*, 301−314. (d) Szterenberg, L.; Latos-Grazyñski, L. *Inorg. Chem.* **1997**, *36*, 6287−6291.

(9) Photoinduced Through-Space Electron-Transfer within Free-Base and Zinc Porphyrin- Containing Poly(Amide) Dendrimers. Rajesh, C. S.; Capitosti, G. J.; Cramer, S. C.; Modarelli, D. A. *J. Phys. Chem. B* **2001**, *105*, 10175−10188. Photoinduced Electron-Transfer within Porphyrin-Containing Poly(Amide) Dendrimers. Capitosti, G. J.; Cramer, S. C.; Rajesh, C. S.; Modarelli, D. A. *Org. Lett.* **2001**, *3*(*11*), 1645−1648.

(10) Strachan, J. P.; Gentemann, J. S.; Kalsbeck, W. A.; Lindsey, J. S.; Holten, D.; Bocian, D. F. *J. Am. Chem. Soc.* **1997**, *119*, 11191.

(11) Geier, G. R., III.; Haynes, D. M.; Lindsey, J. S. *Org. Lett.* **1999**, *1*, 1455−1458.

(12) Becke, A. D. *J. Chem. Phys.* **1993**, *98*, 5648.

(13) Lee, C.; Yang, W.; Parr, R. G. *Phys. Rev. B* **1988**, *37*, 785.

(14) A description of the Gaussian implementation of density functionals can be found in: Johnson, B. G.; Gill, P. M. W. L.; Pople, J. A. *J. Chem. Phys.* **1993**, *98*, 5612.

(15) Frisch, M. J.; Trucks, G. W.; Schlegel, H. B.; Scuseria, G. E.; Robb, M. A.; Cheeseman, J. R.; Zakrzewski, V. G.; Montgomery, J. A., Jr.; Stratmann, R. E.; Burant, J. C.; Dapprich, S.; Millam, J. M.; Daniels, A. D.; Kudin, K. N.; Strain, M. C.; Farkas, O.; Tomasi, J.; Barone, V.; Cossi, M.; Cammi, R.; Mennucci, B.; Pomelli, C.; Adamo, C.; Clifford, S.; Ochterski, J.; Petersson, G. A.; Ayala, P. Y.; Cui, Q.; Morokuma, K.; Malick, D. K.; Rabuck, A. D.; Raghavachari, K.; Foresman, J. B.; Cioslowski, J.; Ortiz, J. V.; Stefanov, B. B.; Liu, G.; Liashenko, A.; Piskorz, P.; Komaromi, I.; Gomperts, R.; Martin, R. L.; Fox, D. J.; Keith, T.; Al-Laham, M. A.; Peng, C. Y.; Nanayakkara, A.; Gonzalez, C.; Challacombe, M.; Gill, P. M. W.; Johnson, B. G.; Chen, W.; Wong, M. W.; Andres, J. L.; Head-Gordon, M.; Replogle, E. S.; Pople, J. A. *Gaussian 98*, revision A.6; Gaussian, Inc.: Pittsburgh, PA, 1998.

(16) Bode, B. M.; Gordon, M. S. *J. Mol. Graphics Mod.* **1998**, *16*, 133.

(17) Schmidt, M. W.; Baldridge, K. K.; Boatz, J. A.; Elbert, S. T.; Gordon, M. S.; Jensen, J. H.; Koseki, S.; Matsunaga, N.; Nguyen, K. A.; Su, S. J.; Windus, T. L.; Dupuis, M.; Montgomery, J. A. *J. Comput. Chem.* **1993**, *14*, 1347.

(18) Marquardt, D. W. *J. Soc. Ind. Appl. Math.* **1963**, *11*, 431.

(19) **1i**: Furuta, H.; Asano, T.; Ogawa, T. *J. Am. Chem. Soc.* **1994**, *116*, 767−8.

(20) **1e**: Furuta, H.; Ishizuka, T.; Osuka, A.; Dejima, H.; Nakagawa, H.; Ishikawa, Y. *J. Am. Chem. Soc.* **2001**, *123*, 6207−6208.

(21) Platt, J. R. *J. Opt. Soc. Am.* **1953**, *43*, 252.

(22) (a) Dorough, G. D.; Shen, K. T. *J. Am. Chem. Soc.* **1950**, *72*, 3939−3944. (b) Dorough, G. D.; Huennekens, F. M. *J. Am. Chem. Soc.* **1952**, *74*, 3974−3976.

(23) Weiss, C. In *The Porphyrins*; Dolphin, D., Ed.; Academic Press: New York, 1978; Vol. III, pp 211−223.

(24) Bookser, B. C.; Bruice, T. C. *J. Am. Chem. Soc.* **1991**, *113*, 4208.

(25) Gradyushko, A. T.; Sevchenko, A. N.; Solvyov, K. N.; Tsvirko, M. P. *Photochem. Photobiol.* **1970**, *11*, 387−400.; Strachan, J.-P.; O'Shea, D. F.; Balasubramanian, T.; Lindsey, J. S. *J. Org. Chem.* **2000**, *65*, 3167.

(26) The radiative rate constant is the product of the oscillator strength and the square of the transition energy. The values of the transition energy are substantially larger for H_2TPP (15504 cm^{-1}) than either **1i** (13777 cm^{-1}) or **1e** (14318 cm^{-1}), resulting in smaller radiative lifetimes for the N-confused porphyrins.

(27) Wolff, S.; Rajesh, C. S.; Capitosti, G. J.; Guerrero, C. D.; Aleman, E.; Cramer, S. J.; Modarelli, D. A. Unpublished results.